

Dynamics of a Complex Quantum Magnet

James W. Landry*

Sandia National Laboratory, Albuquerque, NM 87185

S.N. Coppersmith[†]

Physics Department, University of Wisconsin, 1150 University Ave., Madison, WI 53706

(Dated: November 21, 2018)

We have computed the low energy quantum states and low frequency dynamical susceptibility of complex quantum spin systems in the limit of strong interactions, obtaining exact results for system sizes enormously larger than accessible previously. The ground state is a complex superposition of a substantial fraction of all the classical ground states, and yet the dynamical susceptibility exhibits sharp resonances reminiscent of the behavior of single spins. These results show that strongly interacting quantum systems can organize to generate coherent excitations and shed light on recent experiments demonstrating that coherent excitations are present in a disordered spin liquid [1]. The dependence of the energy spectra on system size differs qualitatively from that of the energy spectra of random undirected bipartite graphs with similar statistics, implying that strong interactions are giving rise to these unusual spectral properties.

The motivation for understanding the dynamics of quantum systems continues to grow as technology miniaturizes. That quantum and classical dynamics differ fundamentally is underscored by the indications that quantum dynamics can be harnessed in the form of quantum computation to solve problems that are intractable using the processes of classical physics [2].

The promise and difficulty of quantum dynamics both arise because the amount of information needed to specify a quantum state grows exponentially with the system size. The number of complex numbers needed to specify a general quantum state of N quantum-mechanical two-state spins (or qubits) is 2^N . A classical computer performing 10^{14} floating point operations per second [3] would take 10^8 years to perform a single operation when $N = 100$ and 10^{21} years when $N = 144$.

Here we study a frustrated spin model that is a quantum generalization of the two-dimensional $\pm J$ Edwards-Anderson (E-A) spin glass model [4], a canonical example of a classical system whose competing interactions give rise to many low-energy states. The essential physical ingredients of the E-A model arise in a wide variety of optimization problems in many fields [5]: the system cannot satisfy simultaneously all its constraints, and many different configurations are equally effective in minimizing the energy. Though the two-dimensional $\pm J$ E-A model is simpler than the three-dimensional version—it is disordered at all nonzero temperatures [6] and individual ground states can be found in a time that scales as a polynomial of the system size [7]—it has a large ground state degeneracy and a complex energy landscape [6, 8, 9]. Motivated by recent experiments on $\text{LiY}_x\text{Ho}_{1-x}\text{F}_4$ that demonstrate that quantum tunneling has profound effects on the dynamics of a three-dimensional Ising spin glass with dipolar couplings [1, 10, 11], we study the

quantum system obtained by adding a small quantum tunneling term to the two-dimensional E-A model.

We calculate numerically exact eigenstates and dynamical response functions of quantum E-A models with up to 144 spins in the limit of strong interaction strength. At low frequencies the excitation spectrum is remarkably sparse. The number of excitations per unit energy at low energies does not vary significantly with system size, even though the number of eigenvalues grows exponentially with system size while the energy bandwidth is only growing polynomially. The eigenvalues and eigenvectors of each realization are obtained by diagonalizing the adjacency matrix of a graph, and we demonstrate that strong correlations play a vital role by comparing the spin glass excitation spectra to spectra of graphs with similar connectivity statistics but randomly chosen connections. These theoretical results provide a natural framework for understanding recent experiments demonstrating the presence of sharp, saturable resonances in the quantum spin liquid $\text{LiY}_{0.955}\text{Ho}_{0.045}\text{F}_4$ [1].

We study two-dimensional systems with periodic boundary conditions in which spin-1/2 spins interact with nearest neighbors on $\sqrt{N} \times \sqrt{N}$ square lattices. The quantum Hamiltonian is

$$H_Q = - \sum_{\langle ij \rangle} J_{ij} \sigma_{i,z} \sigma_{j,z} + \Gamma \sum_i \sigma_{i,x}, \quad (1)$$

where $\sigma_{i,x}$ and $\sigma_{i,z}$ are Pauli matrices: $\sigma_{i,x} = \begin{pmatrix} 0 & 1 \\ 1 & 0 \end{pmatrix}$ and $\sigma_{i,z} = \begin{pmatrix} 1 & 0 \\ 0 & -1 \end{pmatrix}$. The sum $\langle ij \rangle$ is over all nearest neighbor pairs. A given sample has a fixed realization of bonds in which each bond J_{ij} is chosen to be $-J$ and $+J$ with equal probability. This Hamiltonian, which has been studied by many groups [12], is believed to be rele-

vant to the experimental system $\text{LiY}_x\text{Ho}_{1-x}\text{F}_4$ [1, 10, 11], where the coefficient Γ is tunable because it is proportional to an applied transverse magnetic field. The $\Gamma \rightarrow 0$ limit is the two-dimensional $\pm J$ Edwards-Anderson (E-A) model [4].

As $\Gamma/J \rightarrow 0$ the low energy quantum states $|\psi_n\rangle$ become superpositions of states corresponding to ground state configurations $|\alpha\rangle$ of the classical model,

$$|\psi_n\rangle = \sum_{\alpha} c_{\alpha n} |\alpha\rangle. \quad (2)$$

The number of ground states of the classical two-dimensional $\pm J$ E-A model grows with N much more slowly than the number of configurations (though still exponentially) [9, 13]; we use an algorithm that we have developed that finds all the classical ground states efficiently [13] and standard degenerate perturbation theory [14] to compute the low energy quantum states of about 90% of 10×10 realizations and about 40% of 12×12 realizations [15]. In the limit $\Gamma/J \rightarrow 0$, each low energy quantum eigenstate is a superposition of classical ground state configurations related to each other by serial flipping of individual flippable spins, where a flippable spin is one with an equal number of satisfied and unsatisfied bonds [16]. This follows because the matrix element $\langle \alpha | (\sum_i \sigma_{ix}) | \beta \rangle$ of the quantum tunneling term between any two classical configurations corresponding to the quantum basis states $|\alpha\rangle$ and $|\beta\rangle$ is nonzero only if the two states differ by a single spin flip, and, to lowest order, only states $|\alpha\rangle$ and $|\beta\rangle$ with the same energy contribute. The number of flippable spins clearly is no greater than N , the number of spins in the system, so the matrix characterizing the possible transitions between classical ground states is extremely sparse, and thus well-suited for diagonalization using Lanczos techniques [17, 18, 19]. We have computed the dynamical magnetic susceptibility by finding low-energy eigenvalues and eigenstates using the sparse matrix ARPACK numerical library [20] with C++ bindings [21]. Most of the results shown here are for individual realizations; though there are large sample-to-sample variations in the number of ground states for a given system size [13], the qualitative results on which we focus are robust.

The ground state dynamical magnetic susceptibility $\chi''(\omega)$ characterizes the response of a system at zero temperature to a magnetic field applied along the z axis oscillating at frequency ω [22]. The susceptibility consists of sets of Dirac δ -function peaks (that in physical systems spread out into a finite width in frequency due to decoherence processes); each peak occurs at a frequency that is \hbar times the energy difference between an excited state and the ground state. For the $\pm J$ spin glass, as $\Gamma/J \rightarrow 0$ the value of J affects only the energy zero and the susceptibility at frequencies ω satisfying $\hbar\omega \ll J$ depends only on the ratio $\hbar\omega/\Gamma$.

Figure 1 shows the zero temperature dynamic magnetic

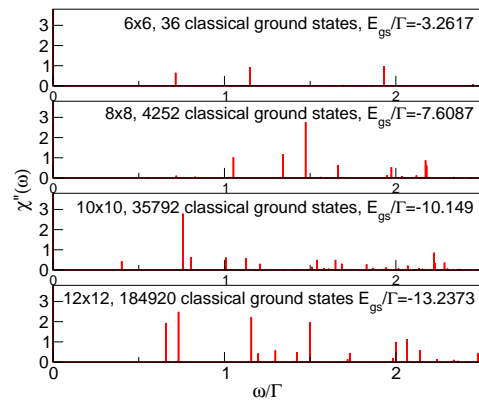


FIG. 1: Zero temperature dynamic magnetic susceptibility $\chi''(\omega)$ of systems of size 6×6 , 8×8 , 10×10 and 12×12 . The peaks in the susceptibility occur at frequencies ω that satisfy $\hbar\omega = E_n - E_0$, where E_n is the energy of an excited state and E_0 is the energy of the ground state. The density of low-energy excitations does not increase appreciably as the system size increases, even though an exponentially increasing number of states are in an energy bandwidth that grows approximately linearly with the system size.

susceptibility of systems of size 6×6 , 8×8 , 10×10 , and 12×12 . The density of low energy excitations increases extremely slowly with system size. This result is surprising because the number of energy eigenvalues grows exponentially with the number of spins N , while these energies all lie within a bandwidth that grows roughly linearly with N .

To obtain context for these results, we interpret the Hamiltonian matrix for the quantum spin glass as the adjacency matrix of an undirected bipartite graph [23, 24, 25] in which each classical ground state is a node and edges connect every pair of classical ground states coupled by the quantum term in the Hamiltonian. The graph is bipartite because the edges connect states that differ by a single spin reversal, one of which has an even and the other an odd number of up spins. The spin glass graphs have a modest number of disconnected pieces, called clusters [26]. Figure 2 compares the density of energy levels of the largest cluster of a 10×10 spin glass realization (with 17040 nodes and 77684 edges) to the density of energy levels of a symmetric bipartite random matrix with 10000 nodes and 50000 edges. The bipartite random matrix has a large energy gap between the ground state and first excited state, and once this gap is exceeded the density of energy levels is much greater than at low energies in the spin glass. The energy level spacing between the excited states of the random matrix is approximately inversely proportional to the number of nodes.

We have compared other properties [27] of the graphs underlying the quantum spin glass to those of random bipartite graphs. The degree distribution [28] describ-

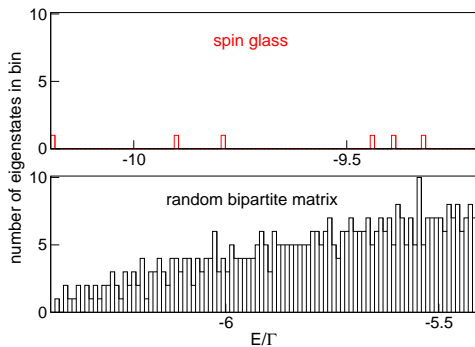


FIG. 2: Density of states as a function of energy at low energies for the largest connected component (with 17040 nodes and 77684 links) of the graph characterizing a 10×10 spin glass realization and of a bipartite random matrix with 10000 nodes and 50000 links. The quantum ground state energy E_0 for the spin glass is $E_0/\Gamma = -10.1949$, and for the bipartite graph $E_0/\Gamma = -10.2335$. The ordinate shows the number of eigenvalues in a bin of width 0.01. The bipartite random matrix has a large gap between the ground state and first excited state, and, once the gap is exceeded, a much larger density of states than the spin glass.

ing the number of links emanating from the nodes of the spin glass graphs is even narrower than the Poisson distribution of a bipartite random graph with the same mean degree. Figure 3 shows the clustering coefficient C [29], which for bipartite graphs is the probability that two nodes with a common second neighbor are themselves second neighbors [30]. The clustering coefficients of spin glass graphs are significantly larger than those of bipartite random graphs with the same number of nodes and edges [30], and are close to those of graphs describing N noninteracting spins, which have 2^N nodes, each node with degree N , and clustering coefficients $C = 4/(N + 1)$ [31].

Though some statistical properties of the spin glass graphs are similar to those of graphs for noninteracting quantum spins, the ground state of the quantum spin glass differs significantly from that of noninteracting quantum spins. Figure 4 (inset) displays the spins in the quantum ground state of a 12×12 system that are fluctuating, in that $|\langle S_{iz} \rangle| \neq 1$, where $\langle S_{iz} \rangle$ is the expectation value of the z th component of the i th spin. The fluctuating spins form connected “bunches” [13] with up to 15 spins, so a description in terms of noninteracting spins is not appropriate. The main panel of Figure 4 shows the participation ratios P_α of different classical ground states in the quantum ground state, where $P_\alpha = |c_{\alpha 0}|^2$, with the $c_{\alpha 0}$ defined in Eq. (2). The spin glass participation ratios vary over several orders of magnitude (note the logarithmic abscissa), while for a system of N noninteracting spins, the participation ratio is $1/2^N$ for all classical configurations. Figure 4 shows that the partici-

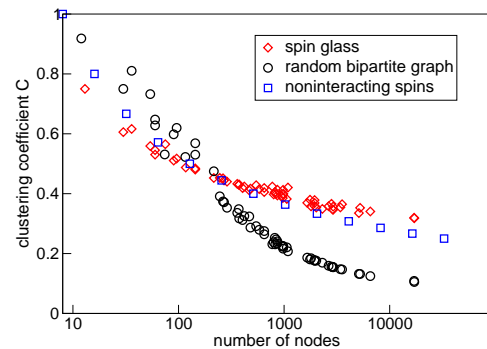


FIG. 3: Clustering coefficients C of spin glass graphs, of bipartite random graphs with the same number of nodes and edges, and of graphs for noninteracting quantum spins, versus number of nodes. The clustering coefficients of the spin glass graphs are significantly larger than those of random bipartite graphs, and close to those of graphs for noninteracting spins.

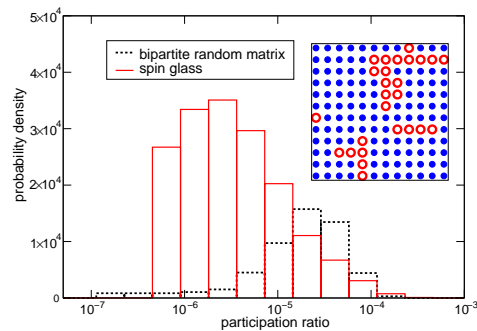


FIG. 4: Histogram of the probability distribution of classical ground states whose participation ratio P_α is in a given range in the quantum ground state, on a logarithmic scale. Here, $P_\alpha = |c_{\alpha 0}|^2$, where the $c_{\alpha n}$ are defined in Eq. (2). The distributions of participation ratios differ significantly between the spin glass and the random bipartite matrix, though in both cases the P_α vary over many orders of magnitude (note the logarithmic abscissa). Inset: Spins denoted with open circles have mean magnetization $\langle S_i \rangle$ satisfying $|\langle S_i \rangle| \neq 1$ in the quantum ground state.

pation ratios of the adjacency matrix of a bipartite random graph also vary over several orders of magnitude, but with quite different statistics.

We expect the perturbative methods we use to be valid so long as the energy arising from the quantum perturbation ($\approx \Gamma N$) is smaller than the energy gap between the classical ground state and lowest classical excited states ($= J$), so that the procedure is valid only for $\Gamma \lesssim J/N$. Exact diagonalizations of very small (3×3 and 4×4) systems are consistent with this expectation.

Our results, particularly the low density of well-defined low-frequency excitations, provide a framework for un-

derstanding the generation of coherent, saturable excitations in a complex quantum spin liquid [1]. Saturability arises naturally when the density of excitations is low because a frequency that induces a transition from the ground state to an excited state will not be able to induce a second transition from the excited state. When external excitations couple only two states, the system will display coherent oscillations and will have the capability of encoding phase-coherent information [1]. An important future goal is to understand how to implement controlled dynamics involving more than two energy levels in this strongly interacting system, as has been achieved in the weakly interacting regime in the context of NMR quantum computation [32].

We have benefited greatly from discussions with J. Brooke, S. Ghosh, T.F. Rosenbaum, and S.A. Trugman. This work was supported by the MRSEC program of the National Science Foundation under Award No. DMR-9808595 at The University of Chicago and by the National Science Foundation under Award No. DMR-0209630. SNC thanks the Aspen Center for Physics for hospitality during the preparation of this manuscript.

* Electronic address: jwlandr@sandia.gov

† Electronic address: snc@physics.wisc.edu

- [1] S. Ghosh, R. Parthasarathy, T. Rosenbaum, and G. Aeppli, *Science* **296**, 2195 (2002).
- [2] M. Nielsen and I. Chuang, *Quantum Computation and Quantum Information* (Cambridge Univ. Press, 2000).
- [3] The world's fastest supercomputer performs slightly fewer than 4×10^{13} floating-point operations per second (<http://www.top500.org/>).
- [4] S. Edwards and P. Anderson, *J. Phys. F* **5**, 965 (1975).
- [5] M. Mezard, G. Parisi, and M. Virasoro, *Spin Glass Theory and Beyond: An Introduction to the Replica Method and Its Applications* (World Scientific, Singapore, 1987).
- [6] M. Palassini and A. Young, *Phys. Rev. B* **63**, 140408(R) (2001).
- [7] L. Bieche, J. Uhry, R. Maynard, and R. Rammal, *J. Phys. A* **13**, 2553 (1980).
- [8] G. Santoro, R. Martonak, E. Tosatti, and R. Car, *Science* **295**, 2427 (2002).
- [9] L. Saul and M. Kardar, *Phys. Rev. E* **48**, R3221 (1993); *Nuc. Phys. B* **432**, 641 (1994).
- [10] J. Brooke, D. Bitko, T. Rosenbaum, and G. Aeppli, *Science* **284**, 779 (1999).
- [11] J. Brooke, T. Rosenbaum, and G. Aeppli, *Nature* **413**, 610 (2001).
- [12] O. Motrunich, S. Mau, D. Huse, and D. Fisher, *Phys. Rev. B* **61**, 1160 (2000), and references therein.
- [13] J. Landry and S. Coppersmith, *Phys. Rev. B* **65**, 134404 (2002).
- [14] R. Shankar, *Principles of quantum mechanics* (Plenum Press, New York, 1980).
- [15] Because the distribution of the number of ground states in different realizations is log-normal, some randomly-generated realizations have extremely large numbers of ground states. Computational limitations prevent us

from generating all the the ground states of these realizations in a reasonable amount of time [13].

- [16] S. Coppersmith, *Phys. Rev. Lett.* **67**, 2315 (1991).
- [17] J. Cullum and R. Willoughby, *Lanczos algorithms for large symmetric eigenvalue computations: Theory* (Birkhauser, Boston, MA, 1985).
- [18] E. Dagotto, *Rev. Mod. Phys.* **66**, 763 (1994).
- [19] C. Lanczos, *Linear Differential Operators (Classics in Applied Mathematics, 18)* (Society for Industrial and Applied Mathematics, 1996).
- [20] R. Lehoucq, K. Maschhoff, D. Sorensen, and C. Yang, <http://www.caam.rice.edu/software/ARPACK/>.
- [21] S. Shaw, monsoon.harvard.edu/~shaw/programs/lapack.html.
- [22] The ground state dynamical magnetic susceptibility is

$$\chi''(\omega) = \sum_n |\langle \psi_n | M_z | \psi_0 \rangle|^2 \delta(\omega - \omega_{n0}),$$

where the sum is over quantum energy eigenstates $|\psi_n\rangle$, $|\psi_0\rangle$ is the quantum ground state, $\hbar\omega_{n0} = (E_n - E_0)$ is the energy difference between the states $|\psi_n\rangle$ and $|\psi_0\rangle$, and $M_z = \sum_\alpha \sigma_{\alpha z}$ is the z -component of the total magnetization (see, e.g., E.R. Gagliano and C.A. Balseiro, *Phys. Rev. B* **38**, 11766 (1988)).

- [23] G. Chartrand, *Introductory Graph Theory* (Dover, New York, 1985).
- [24] D. Cvetkovic, M. Doob, and H. Sachs, *Spectra of graphs: theory and application* (Academic Press, New York, 1980).
- [25] I. Farkas, I. Derenyi, A.-L. Barabasi, and T. Vicsek, *Phys. Rev. E* **64**, 026704:1 (2001), cond-mat/0102335.
- [26] A. Hartmann, *Phys. Rev. E* **63**, 016106 (2001).
- [27] R. Albert and A.-L. Barabasi, *Rev. Mod. Phys.* **74**, 47 (2002).
- [28] A.-L. Barabasi and R. Albert, *Science* **286**, 509 (1999).
- [29] D. Watts and S. Strogatz, *Nature* **393**, 440 (1998).
- [30] M. Newman, S. Strogatz, and D. Watts, *Phys. Rev. E* **64**, 026118 (2001).
- [31] To calculate the clustering coefficient C for the graph for noninteracting quantum spins, consider two distinct second neighbors of a given reference state (there are $\frac{1}{2} [\frac{1}{2}N(N-1)] [\frac{1}{2}N(N-1) - 1]$ of such pairs). Note that each state in the pair has two spins that differ from the reference state, and that they are second neighbors to each other if one of these spins is in common. For a given reference state, there are $N(N-1)/2$ ways to choose the first state of the pair. If the second state of the pair is a second neighbor, then one of the two flipped spins is the same in the second state of the pair also. There are $N-2$ possible locations of the second flipped spin in the second state, since it can be anywhere except for the locations of the two flipped spins of the first state of the pair. Each pair is counted twice by this process, so the number of ways to choose a pair of states that are second neighbors to each other as well as the reference state is $[\frac{1}{2}] [\frac{1}{2}N(N-1)] [2] [N-2]$, and the clustering coefficient C is

$$C = \frac{[\frac{1}{2}] [\frac{1}{2}N(N-1)] [2] [N-2]}{\frac{1}{2} [\frac{1}{2}N(N-1)] [\frac{1}{2}N(N-1) - 1]} = \frac{4}{N+1}. \quad (3)$$
- [32] D.G. Cory, A.F. Fahmy, and T.F. Havel, *PNAS (USA)* **94**, 1634 (1997); N.A. Gershenfeld and I.L. Chuang, *Science* **275**, 350 (1997).